MAGNETIC AND DIELECTRIC STUDIES OF IRON NANOPARTICLES

[1]P.Durga Prasad, [2]P Siva Prasada Reddy, [3]Atnafu Guadie Assefa, [4]G.Nageswara Rao*
[1]Research Scholar, [2] Research Scholar, [3]Research Scholar, [4]Professor
[1]Department of Inorganic & Analytical Chemistry,
[1]Andhra University, Visakhapatnam, India

Abstract : Iron nanoparticles were synthesized by sol-gel protocol. The techniques of XRD, FTIR, RAMAN, SEM, EDX, and VSM were used to characterize the ferrite nanoparticles. Through the characterization of the prepared iron nanoparticles, the effect of annealing temperature, chemical composition and preparation technique on the microstructure, magnetization and the particle size of the ferrite nanoparticles are discussed.XRD results clearly show that the lattice parameter and crystallite size are increased with annealing temperature. SEM photograph of the sample shows the shape of the particles is almost spherical. The magnetic properties of the iron oxide magnetite nanoparticles were investigated with a Vibrating Sample Magnetometer. Magnetic measurements at room temperature showed improvements in the saturation magnetization with increase in annealing temperature, which might be related to increase in particle size. Dielectric constant and dielectric loss were observed. The effect of annealing temperature on the magnetic properties of the samples is analyzed by vibrating sample magnetometer (VSM) and Dielectric properties are also measured.

Keywords: Vibrating Sample Magnetometer, Dielectric constant, dielectric loss, SEM, XRD.

1. Introduction:

Iron nanoparticles are found to be exhibiting interesting structural and magnetic properties. The possible applications of the iron nanoparticles are in magnetic storage, as precursors for ferro fluids, magnetic guided drug delivery agents and gas sensor [1]. In recent years, the utilization of iron oxide nanoparticles with novel properties and functions has been widely studied due to their nano-range size, high surface area to volume ratios and superparamagnetism. [2-5]. Most of iron oxides show semiconductor properties with narrow band gap (2.0–2.3 eV) and are photoactive under solar irradiation as photo catalysts absorbing visible light.[6,7] For example, Fe_2O_3 with band-gap of 2.2 eV is an interesting n-type semiconducting material and a suitable candidate for photo degradation under visible light condition.

The magnetic particles with smaller size become single domain in contrast with the usual multi domain structure for bulk magnetic material exhibiting super paramagnetization. Magnetic nanoparticles exhibiting super paramagnetic behaviour display higher saturation magnetization and low coercivity having potential applications viz., as magnetic resonance imaging contrast agents in ferro fluids based technology, information storage device [8,9]. Nanostructuring of materials has opened up a new dimension and made size as a parameter to be considered for the phase diagrams in addition to the existing ones. The properties of nanosized semiconductor particles have been known to depend very sensitively on the particle size [10]. The physical properties of semiconductor nanocrystals are dominated by the spatial confinement of excitations (electronic and vibrational). Quantum confinement that manifests itself in widening of HOMO, LUMO gap or the bandgap increase with decreasing crystallite size and its implications on the electronic structure and photo physics of the crystallites has generated considerable interest [11]. In order to synthesize nanoparticles and retain the size and morphology, it is mandatory to try and maintain sufficiently low temperatures during synthesis, processing and also in the course of application.

Magnetic particles with sizes in the nanometer scale are now of interest because of their many technological applications and unique magnetic properties which differ considerably from those of bulk materials. Below a critical size, magnetic particles become single domain in contrast with the usual multi domain structure of the bulk magnetic materials exhibiting unique phenomena such as super paramagnetic and quantum tunneling of the magnetization [12]. Dielectric materials are changed as the particle size decreases from a typical bulk value into a nanometer scale.

2. Synthesis:

3.2 gm of PEG taken in 25 ml of D.H_2O and stirred. 3.3 gm of Fe $(SO_4).7H_2O$ in 10 ml of D.H_2O, 9.6 gm of Fe_2 $(SO_4)_3$ in 20 ml of D.H_2O are stirred separately. Now both Fe $(SO_4).7H_2O$ and Fe_2 $(SO_4)_3$ Solutions are added drop by drop into the PEG solution. Then the solution is stirred for 30mins, Ammonia solution is added for maintain pH-10. The mixture was further stirred for 4hrs and filtered, washed with D.I. water and finally rinsed with acetone, dried in hot air oven at 60^oC/ 8h. The dried compound was calcined at different temperatures at 400^oC 600^oC and 800^oC for 4hrs to get Fe_3O_4 nanoparticles.

3. Results and Discussion:

3.1. X-Ray Diffraction Spectra:

XRD patterns of Fe_3O_4 nanoparticles as-synthesized and calcined at different temperatures at 400ºC, 600ºC, 800ºC. From the patterns of samples, it was found that all the different peaks at (110), (024) and (116) corresponds to36 º, 52 º and 55º.

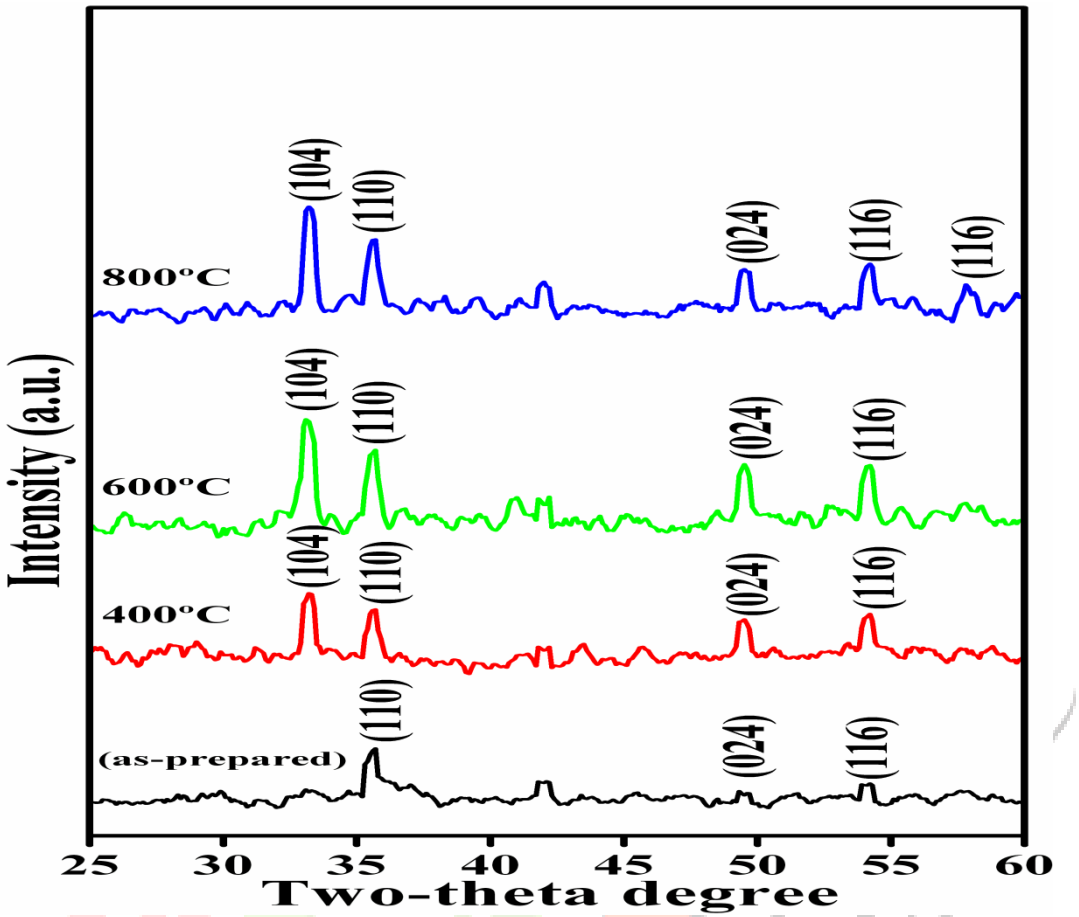

Fig.1 XRD patterns of Fe_3O_4 nanoparticles as-synthesized and calcined samples at 400ºC, 600ºC, 800ºC.

For calcined samples we observed peaks (104), (110), (024) and (116), are well indexed at 30º, 36 º, 52º and 55º to the inverse cubic spinel structure of Fe_3O_4. In the above spectra phase identification is one of the most important uses in XRD. As shown in fig XRD pattern of Fe_3O_4 nanoparticles after annealing the XRD patterns well indexed to the cubical spinel phase of magnetite and no other peaks observed in as synthesized material.

3.2 FTIR spectra:

The typical FTIR spectra of Fe_3O_4 nanoparticles is shown in fig Broad peak between 3151-3448 cm^{-1} corresponds to O-H stretch vibration and 530-572 cm^{-1} Fe-O-Fe stretching vibration are observed in all the spectra.

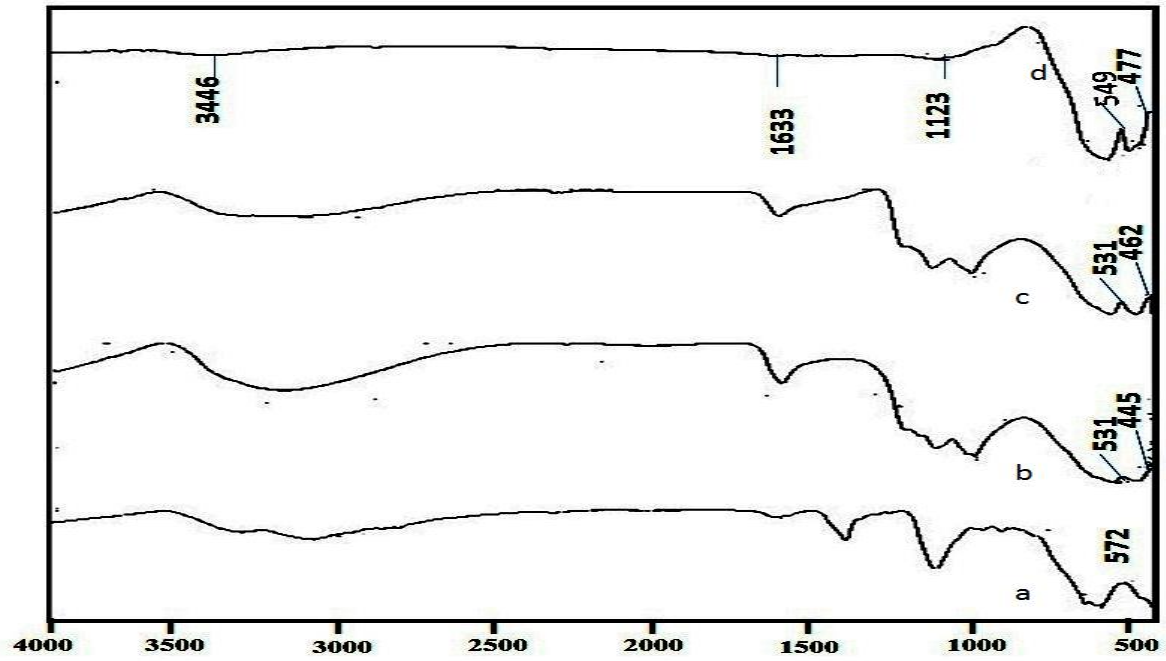

Fig. 2: a) As- Synthesized Fe3o4 nanoparticles. **(b-d)** Illustrates the FTIR spectra of fe3o4 nanoparticles annealed at different temperatures.

Peak observed between 1518-1732 cm^{-1} corresponds to C=O stretching vibration are observed in all the spectra, which are characteristic of asymmetric ν_{as} (COO^-) and the symmetric ν_{as} (COO^-) stretch This explains that the bonding pattern of the carboxylic acid on the surface of nanoparticles was a combination of molecules bonded symmetrically and molecules bonded at an angle to the surface. Peaks observed between 445-475cm^{-1} correspondings to Fe-O(α-Fe_2O_3)observed in all the calcined samples as shown in fig (b-d).

3.3 Raman spectra

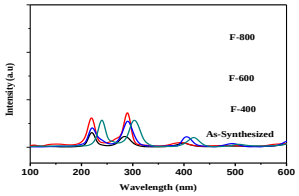

Fig 3. The Raman Spectra of Fe_3O_4 magnetite nanoparticles

Fig.3. Illustrates the raman spectra of Fe_3O_4 magnetite nanoparticles for as-synthesized material and calcined at different temperature, peak observed at 220cm^{-1} ,290cm^{-1},400cm^{-1} ,490,cm^{-1} ,610cm^{-1}, 650cm^{-1} and 720cm^{-1} correspond to Fe_3O_4 vibration mode for as synthesized material and calcined at 400^oC and 600^oC temperature , low intense peak at 610cm^{-1} , 720cm^{-1} correspond to Fe_3O_4 .Calcined at 800°c high intense peak at 240 cm^{-1},290 cm^{-1} and low intense peak at 420 cm^{-1},510 cm^{-1},620 cm^{-1} and 670 cm^{-1}

correspond to Fe_2O_3.indicating Fe_3O_4 transformation in to Fe_2O_3.these results well match with our XRD results.

3.4 SEM-EDX:

The scanning electron microscope (SEM) is a type of electron microscope that images the sample surface by scanning it with a high-energy beam of electrons in a raster scan pattern. The electrons interact with the atoms that make up the sample producing signals that contain information about the sample's surface topography as shown in Fig.4. Fig.4.(a,b) are as prepared samples with spherical structure, Fig.4.(c,d) are calcined at 400ºC with Spherical structure, Fig.4.(e,f) are calcined at 600ºC with Spherical structure and Fig.4.(g,h) are calcined at 800ºC with Sphere structure. The EDX analysis shown in Fig.4.(i) confirms the presence of Fe and O, the consequent elements of F-400.

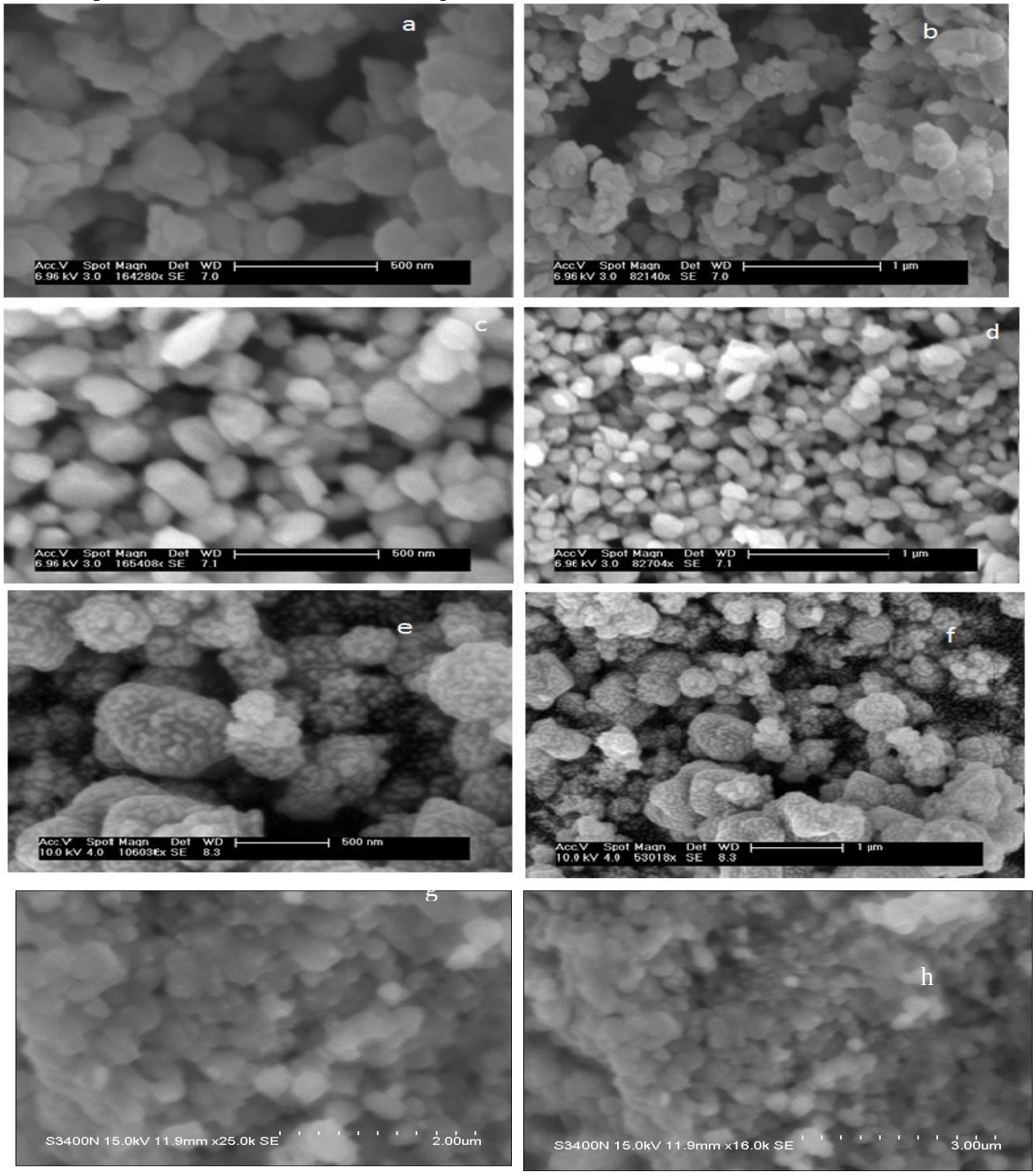

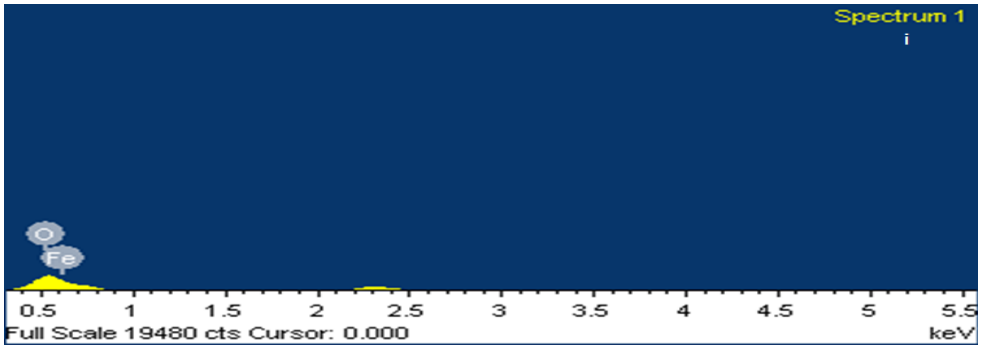

Fig.4 SEM images of Fe_3O_4 nanoparticles (a,b) as-synthesized and calcined at different temperatures at(c,d) 400ºC, (e,f) 600ºC and (g, h) 800ºC, (i) EDX Spectrum of F-400.

DIELECTRIC PROPERTITES

Dielectric properties of solids are determined by electric dipoles having a length scale of a few angstroms. A local change in microstructure or composition within this length scale affects the type and intensity of the dipole. As the particle size decreases to the nanometer scale local microstructure and composition changes relative to the bulk state are greatly increased especially at the particle surfaces. Consequently, the dielectric properties of nanometer-sized particles are unique and different than those of bulk-sized particles. Fabrication methods of nanometer-sized particles have been developed to a mature state where high control on size and composition is achievable which enables efficient usage of their unique dielectric properties.

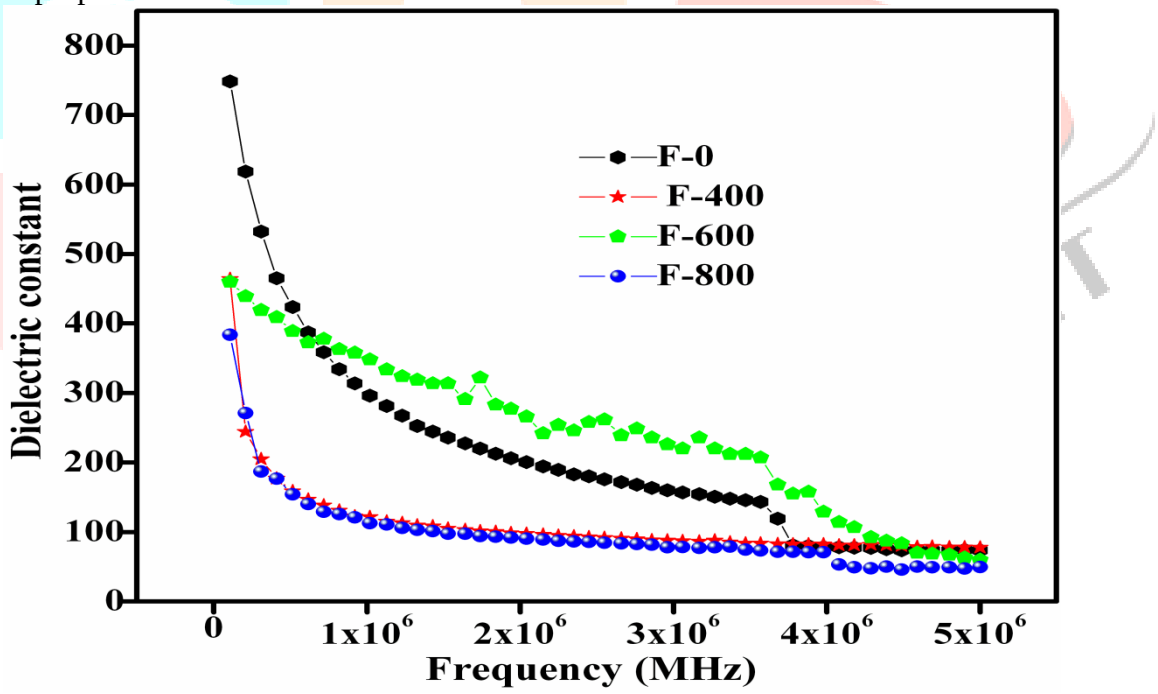

Fig.5 Dielectric constant of Fe_3O_4 nanoparticles as-synthesized and calcined at different temperatures at 400ºC, 600ºC and 800ºC.

The dielectric properties were measured for the samples prepared and impedance analyzer infrequency range of 50Hzto1MHz.The variation in dielectric constant of Fe_3O_4 nanoparticles as-synthesized and calcined at different temperatures at 400ºC, 600ºC, 800ºC. The maximum value of the dielectric constant in the range 380–750 is obtained. From results it is found that the particle size of the material increases with increase in the annealing temperature. According to Koops the decrease in dielectric constant for increase in frequency can be expressed by considering the solid as composed of well conducting grains which is separated by the poorly conducting grain boundaries [13].

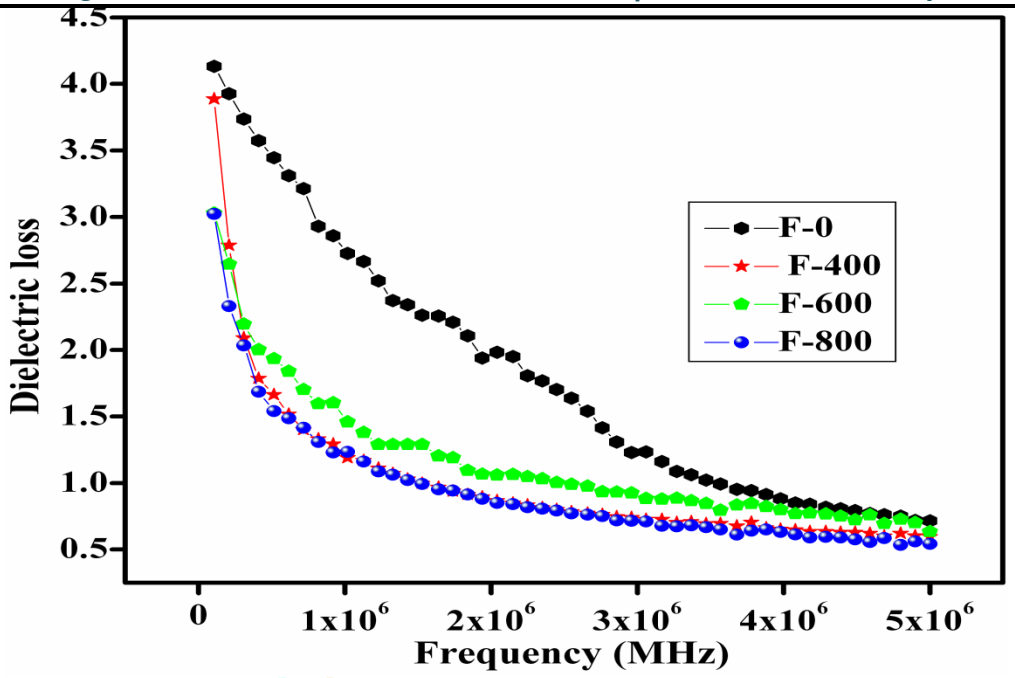

Fig.6 Dielectric loss of Fe_3O_4 nanoparticles as-synthesized and calcined at different temperatures at 400ºC, 600ºC and 800ºC.

The hope of electrons to reach the grain boundary and if the resistance of grain boundary is high enough then electrons pile up at the grain boundaries which causes polarization. The further increase of applied field shows that the electrons reverse their direction of motion and reduces the chance of electrons to approach the grain boundary and decreases the polarization. Thus this study reveals that the value of dielectric constants lowly decreases at lower frequencies and remains constant at higher frequencies [14]. The dielectric constant and dielectric loss decrease as the frequency increases. This decrease indicates the normal behavior of ferrite samples. The decrease takes place when the jumping frequency of electric charge carriers cannot follow the alteration of applied AC electric field beyond a certain critical frequency [15].

VSM STUDIES

Magnetic measurements have been carried out by using quantum design vibrating sample magnetometer. The M–H hysteresis loops of Fe_3O_4 derived under different magnetic field strength demonstrates that both samples are super paramagnetic and different magnetic field intensity does not change the superparamagnetism of nanoparticles. The particle size has been reported to influence the magnetic properties of materials. The particle is size low and the saturation magnetization is large.

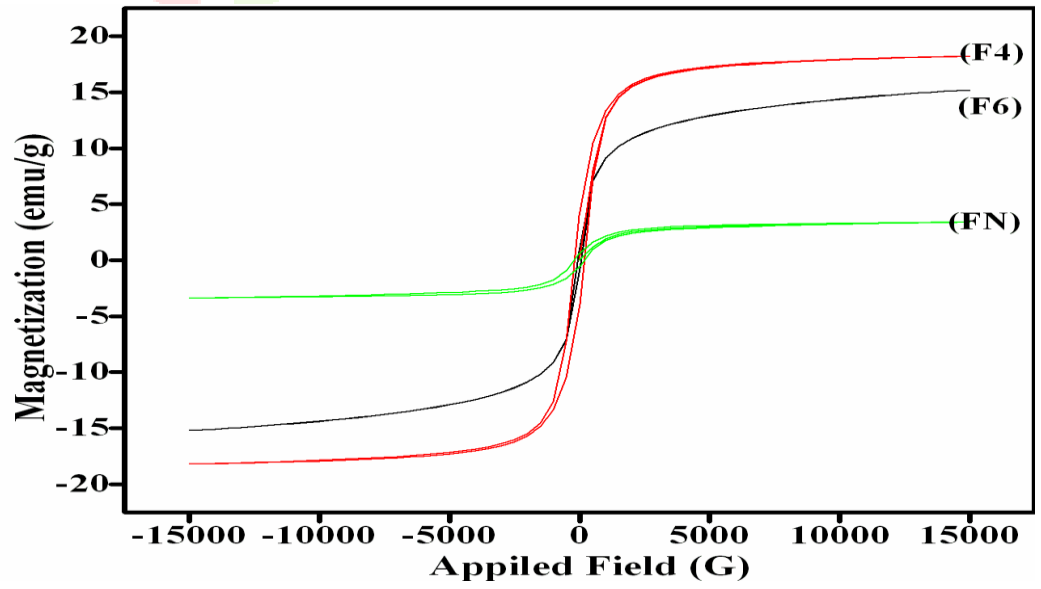

Fig.7 Magnetic studies of Fe_3O_4 nanoparticles as-synthesized and calcined at different temperatures at 400ºC, 600ºC.

A comparison between the magnetic properties before and after annealing, presented in Fig. The magnitudes of Ms and Mr should be scaled by the fraction of the ferrite phase presenting each sample since the impurity phase of hematite is a canted antiferromagnetic at room temperature with only feeble magnetism. The increase in the magnetization with increase in the annealing temperature is very likely related to increase in the particle size. This size dependent effect has been well established in magnetite nanoparticles where it was interpreted in terms of the presence of magnetic dead layer on the surface of a nanoparticle [16].

Due to the strong molecular field, ferro- and ferromagnetic materials are self-saturating, or "spontaneously magnetized" in the absence of an external field. However, it is still easy to find a ferro- or ferrimagnetic sample in the unmagnetized state. This is because ferro- and ferrimagnetic contain many small regions, called "domains," which are spontaneously magnetized to saturation *Ms* but oriented at different directions to minimize the energy potential within the material. The *Ms* in these domains cancel each other, yielding zero macroscopic magnetization. When an external field is applied, these domains align with the field, and a large magnetization is observed.

Conclusion:

The syntheses of Iron nanoparticles are synthesized via sol-gel protocol. The structural morphology of the Iron nanoparticles are identified by using SEM which are spherical in nature with particle size 0f~ 100 nm and crystal structure are measured by X-Ray diffraction. Among the four samples of iron nanoparticles calcined at 400^{o}C show better results in all the characterizations and also in dielectric and magnetic studies.

Acknowledgement:

The authors gratefully acknowledge to UGC-NEWDELHI for financial assistance and acknowledge DST-FIST for instrument laboratory, department of inorganic and analytical chemistry for providing instrumentation facility.

References:

1. E. RanjithKumar , P.SivaPrasadaReddy , G.SaralaDevi , S.Sathiyaraj, Journal of Magnetism and Magnetic Materials , (2016) 398 ,281–288.
2. S. A. C. Carabineiro, N. Bogdanchikova, P. B. Tavares and J. L. Figueiredo, RSC Adv., (2012), 2, 2957–2965.
3. M. Niu, F. Huang, L. Cui, P. Huang, Y. Yu and Y. Wang, ACS Nano, (2010), 4, 681–688.
4. P. Xu, G. M. Zeng, D. L. Huang, C. Lai, M. H. Zhao, Z. Wei, N. J. Li, C. Huang and G. X. Xie,Chem. Eng. J., (2012), 203,423–431.
5. J. L. Gong, B. Wang, G. M. Zeng, C. P. Yang, C. G. Niu, Q. Y. Niu, W. J. Zhou and Y. Liang, J. Hazard. Mater. (2009), 164, 1517–1522.
6. J. K. Leland and A. J. Bard, J. Phys. Chem., (1987), 91, 5076– 5083.
7. X. H. Feng, H. J. Guo, K. Patel, H. Zhou and X. Lou, Chem. Eng. J., (2014), 244, 327–334.
8. O.K. Varghese, C.A. Grimes, Metal oxide nanoarchitectures for environmentalsensing, J. Nanoscience. Nanotechnol. (2003), 3, 277–293.
9. R.B. Kamble, V.L. Mathe, Nanocrystalline nickel ferrite thick film as anefficient gas sensor at room temperature, Sens. Actuators B (2008), 131,205–209.
10. A.L. Linsebigler, G. Lu Jr., J.T. Yatus, J. Phys. Chem. (1995),99 7626–7631.
11. A. Fujishima, K. Honda, Nature (1972),238, 37–38.
12. Y L N Murthy, I V Kasi Viswanath, T. Kondala Rao, Rajendra Singh, Int. J. of Chem Tech Research CODEN (USA): IJCRGG ISSN: 0974-4290, ,(2009),Vol.1, No.4, pp 1308-1311.
13. C.G.Koops, PhysRev.83(1951)121.
14.S.R.Kulkarni,C.M.Kanamadi,B.K.Chougule, Mater. Res.Bull.(2005),40, 2064–2072.
15. A.M.Abdeen, ,J.Magn.Magn.Mater. 192 (1999)121.
16. P. Dutta, S. Pal, M.S. Seehra, N. Shah, G.P. Huffman, J. Appl. Phys. 105 (2009),501.